

Polymer Chemistry

Accepted Manuscript



This is an *Accepted Manuscript*, which has been through the Royal Society of Chemistry peer review process and has been accepted for publication.

Accepted Manuscripts are published online shortly after acceptance, before technical editing, formatting and proof reading. Using this free service, authors can make their results available to the community, in citable form, before we publish the edited article. We will replace this *Accepted Manuscript* with the edited and formatted *Advance Article* as soon as it is available.

You can find more information about *Accepted Manuscripts* in the [Information for Authors](#).

Please note that technical editing may introduce minor changes to the text and/or graphics, which may alter content. The journal's standard [Terms & Conditions](#) and the [Ethical guidelines](#) still apply. In no event shall the Royal Society of Chemistry be held responsible for any errors or omissions in this *Accepted Manuscript* or any consequences arising from the use of any information it contains.

Tunable Doubly Responsive UCST-Type Phosphonium Poly(ionic liquid): A Thermosensitive Dispersant for Carbon Nanotubes

Yajnaseni Biswas, Tanmoy Maji, Madhab Dule and Tarun K. Mandal*

Abstract

A phosphonium poly(ionic liquid) (PIL), poly(triphenyl-4-vinylbenzylphosphonium chloride) (P[VBTP][Cl]) of varying and controllable molecular weights are synthesized via reversible addition-fragmentation chain transfer (RAFT) polymerization to afford doubly responsive PIL that respond to both halide ion and temperature. The addition halide ions transforms the transparent aqueous PIL solution into a turbid two-phase solution, forming insoluble microgel aggregates owing to the screening of the positively charged phosphonium groups of PILs and eventually forms intra- and/or inter-chain cross-linking among PIL chains through halide ion bridges. Further, this turbid solution exhibits a distinct upper critical solution temperature (UCST)-type phase transition and transforms into a one-phase transparent solution due to disruption of ion bridges upon heating. The rate of aggregation of P[VBTP][Cl] increases sharply with increase of the size of the added halide ions in this order $I^- > Br^- > Cl^-$. The cloud point temperature (T_{cp}) increases linearly with increasing halide ion concentration. The T_{cp} also increases with increasing molecular weights of the PIL. The phase diagram of aqueous PIL solution shows a highest T_{cp} at 6 wt%. Interestingly, the T_{cp} of the P[VBTP][Cl] in water decreases sharply with addition of small but increasing amount of organic cosolvents. This PIL exhibits very good stabilizing ability for carbon nanotubes in water, whose dispersion state can be switched from dispersed to agglomerate and vice versa by adding halide ion and increasing temperature respectively. The cross-linked hydrogel of P[VBTP][Cl] also shows dual responsiveness towards both halide ion and temperature.

Introduction

Considerable developments in the area of ionic liquids (ILs) have occurred during the past two decades. Of them, poly(ionic liquid)s (PILs), a distinctive subclass of polyelectrolytes, bearing IL species in each repeating monomer unit, have gained considerable attention of late to the polymer and materials science community because of their wide range of applications.¹⁻⁵ The combination of the novel properties of ILs with the improved mechanical durability and dimensional control resulting from polymerization makes PILs a versatile polymeric materials for a variety of applications such as CO₂ sorbents, dispersants, porous materials, thermoresponsive materials, carbon precursors, catalytic materials, and many more.⁶⁻¹⁴

During past two decades, there has been lot of efforts in developing “smart” materials which are responsive to single or multiple stimuli such as temperature, pH, ionic strength etc. for more sophisticated applications.^{15, 16} Among them, thermoresponsive polymers are one of such important smart materials that exhibit a drastic changes in their solution properties upon small changes in temperature.^{17,18} Due to the fast on off switching phase behavior, thermoresponsive polymers can be employed as polymeric carriers to deliver drugs,¹⁹ thermally switchable optical device,²⁰ tissue engineering^{21, 22} etc. Till to date, most of the reported water soluble thermosensitive polymers exhibit either a lower critical solution temperature (LCST)-type or an upper critical solution temperature (UCST)-type phase transition. Some well-studied LCST polymers include poly(*N*-isopropyl acrylamide) (PNIPAM),²³ poly(vinyl ether)s,^{24,25} poly(oxazoline)s²⁶ etc. In contrast, UCST polymers are relatively uncommon. It is known that polymers showing UCST-type phase transition in solution must have a stronger polymer-polymer interaction through hydrogen bonding and/or electrostatic interaction than polymer-solvent interaction at lower temperature. Until today, poly(acrylic acid) (PAA)/poly(acryl amide) (PAm) system is one of the most investigated

UCST-polymer system in water, in which PAA interacts with PAm via hydrogen bonding at low pH.²⁷ Muller et al. have observed that poly(dimethylaminoethyl methacrylate) (PDMAEMA), a typical LCST-type polymer, exhibited dual responsiveness in terms of formation of precipitate (soluble-insoluble transition) in presence of trivalent counter ion at low temperature followed by an insoluble-soluble UCST-type transition upon heating.²⁸ According to them, such precipitation was due to polymer chain-chain interactions arising from electrostatic bridging between the charged segments of polymer. Maruyama et al. have observed that the polymers with ureido groups exhibited UCST-type phase behavior under physiological conditions in the presence of NaCl.²⁹ Aoshima et al. reported that cationic PILs; poly(vinyl ether)s with imidazolium or pyridinium salt pendants exhibited both LCST-type and UCST-type transitions in organic solvent and in water respectively in presence of different counter anions.¹⁸ Recently, we discovered a L-serine-based zwitterionic polymer, synthesised by RAFT-polymerization, exhibiting dual pH and thermoresponsiveness with tunable UCST-type phase transition.³⁰ Beside these studies, there is a nice review by Agarwal et al. that describes a detailed study of a list of existing UCST polymers and copolymers with an aim to design new UCST-type polymeric systems in water.¹⁷ However, in this context, the stimuli-responsiveness of PILs was comparably much less studied in solution. Thus, it would be interesting to design new PILs or screen the existing PILs with an expectation that they would exhibit stimuli-responsiveness, in particular thermoresponsiveness in solution.

Detail survey of literature showed that there were only very few PIL systems that exhibited thermoresponsive property.³¹⁻³⁴ For example, Ritter et al. observed that poly[1-butyl-3-vinylimidazolium bis(trifluoromethanesulfonyl)-imide] showed a pseudo-LCST effect in aqueous solution in the presence of cyclodextrin due the temperature sensitive formation/disruption of its inclusion complex.³¹ The discovery of a LCST-type anionic PIL,

poly(4-tetrabutylphosphonium styrene sulfonate) (PTPSS) in aqueous solution by Ohno et al. further enriched this area.³³ Recently, a cationic PIL, poly(tributyl-4-vinylbenzylphosphonium pentanesulfonate) was found to show the similar LCST-type transition in aqueous solution.³⁵ Thus, it is apparent that phosphonium-based PILs showed mostly LCST-type behavior in water. Although Tenhu et al. observed an UCST-type phase behaviors of imidazolium- and DMAEMA-based polycations in aqueous solution in presence of both LiNTf_2 and NaCl salts.³² But, as per our knowledge, there has not been any report of phosphonium-based PILs exhibiting UCST-type phase behavior in water alone or in presence of any added salts.

Other than the stimuli-responsiveness of PILs, it has been reported earlier that that imidazolium-based ILs/PILs can be widely utilized as dispersants for carbon nanostructures.^{8, 36-39} The stabilizing action of ILs/PILs was observed due to their anchoring on the surface of carbon nanotubes (CNTs) through cation- π interaction.⁴⁰ Thus, it would be interesting to explore the possibility of use of newly designed phosphonium PIL as dispersant for such carbon nanostructures and to study the stimuli-responsiveness of these PIL-based carbon nanostructures composites if there are any.

In this manuscript, we demonstrate the first observation of double responsive behaviors of a designed phosphonium-based PIL, poly(triphenyl-4-vinylbenzylphosphonium chloride) (P[VBTP][Cl]) towards halide ions and temperature (UCST-type) in an aqueous solution. P[VBTP][Cl]s of varying molecular weights are achieved by reversible addition-fragmentation chain transfer (RAFT) polymerization of an IL monomer, [VBTP][Cl]. It is observed that the transparent aqueous solution of P[VBTP][Cl] becomes cloudy upon addition of sodium halide salts such as NaCl , NaBr and NaI . Such cloudy solution becomes transparent above a certain temperature (cloud point) and this is totally reversible and can be easily tuned by the variation of polymer concentration, molecular weight, nature of halide

salts and ionic strength of the medium. We further investigate the thermoresponsiveness of a cross-linked P[VBTP][Cl] hydrogel in presence of NaCl for its applicability as potential “smart” materials for futuristic applications. Moreover, this P[VBTP][Cl] is also used to stabilize multiwall carbon nanotubes (MWCNTs) in aqueous dispersion. Interestingly, the P[VBTP][Cl] stabilized MWCNTs’ dispersion becomes thermoresponsive in presence of NaCl. Therefore, such thermally switchable properties of this new PIL boost the toolbox of thermoresponsive polymers.

Experimental

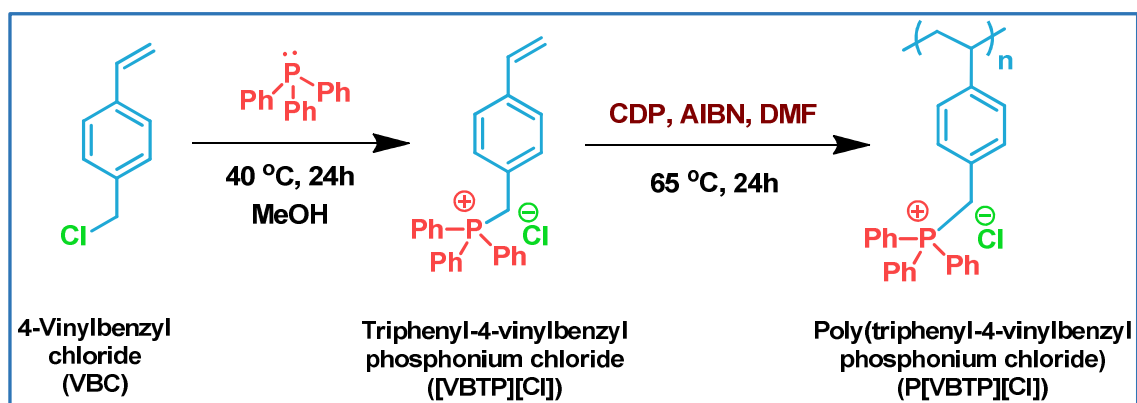
Materials

Triphenylphosphine (TPP, $\geq 95\%$), 4,4'-azobis(4-cyanovaleric acid) (ACVA) and 2,2'-azobis(2-methylpropionitrile) (AIBN, 98%) were purchased from Sigma-Aldrich and were recrystallized twice from ethanol prior to use. 4-Vinylbenzyl chloride (VBC) (Aldrich, 90%) was obtained from Sigma-Aldrich and purified by passing through neutral alumina column to remove inhibitors before use. 4-Cyano-4-[(dodecylsulfanylthiocarbonyl) sulfanyl] pentanoic acid (CDP) (Aldrich, $\geq 97\%$, HPLC), N, N'-methylenebis(acrylamide) (BIS, 99%) and multiwall carbon nanotubes (MWCNTs) (D ~110-170 nm, L ~ 5-9 μm , purity 90+%) were used as received from Sigma-Aldrich. Dimethylformamide (DMF) was dried overnight over CaCl_2 and distilled with CaH_2 under reduced pressure prior to use. Dichloromethane (DCM), acetone, hexane, methanol (MeOH), dimethyl sulfoxide (DMSO) were used as received from E. Merck, India. Milli-Q water was used in preparation of various solutions.

Synthesis of triphenyl-4-vinylbenzylphosphonium chloride ([VBTP][Cl]) monomer

An IL monomer, [VBTP][Cl] was synthesized by nucleophilic substitution reaction between 4-vinylbenzyl chloride (VBC) and triphenylphosphine (TPP) in a molar ratio of 2:1 at 40 °C as shown in Scheme 1. Typically, a 100 mL round-bottom flask was charged with TPP

(5.5836g; 21.3 mmol), VBC (6 mL; 42.57 mmol) and 6 mL of dry MeOH and the reaction mixture was placed in a preheated oil bath at 40 °C and continued heating for 24 h. After completion of the reaction, MeOH was evaporated in a rotary evaporator and the entire liquid mass was dissolved in DCM. Finally, the IL monomer was isolated by precipitation in excess hexane. The process was repeated twice for purification. Finally, the as-prepared purified solid IL, [VBTP][Cl] was kept in a refrigerator under argon atmosphere for subsequent polymerization.



Scheme 1: Synthesis of [VBTP][Cl] monomer and P[VBTP][Cl].

Synthesis of poly(triphenyl-4-vinylbenzylphosphonium chloride) (P[VBTP][Cl]) via RAFT polymerization

The RAFT polymerization of [VBTP][Cl] monomer, was conducted using CDP as a chain transfer agent (CTA). In a typical procedure, 1 g (2.635 mmol) of [VBTP][Cl], 3.89 mg (0.0175 mmol) of CDP and 0.577 mg (3.5138 μ mol) of AIBN were placed in a long neck 25 mL RB flask followed by the addition of 4 mL dry DMF. The reaction mixture was purged with argon gas for 45 min. After that, the container was immediately sealed with silicone rubber septum and stirred in an oil bath thermostated at 65 °C for 24 h. The reaction mixture was then allowed to cool down to room temperature followed by its precipitation in acetone. The obtained white precipitate was redissolved in water and precipitated again in acetone.

Further, the aqueous P[VBTP][Cl] solution was purified by extensive dialysis against double distilled water. The aqueous solution was then lyophilized to obtain a white spongy PIL, which was designated as P[VBTP][Cl]-40K (Table 1). The PILs of two other molecular weights (P[VBTP][Cl]-25K and P[VBTP][Cl]-18K) were prepared just by the variation of $[[\text{VBTP}][\text{Cl}]]_0/[\text{CDP}]_0$ ratios following the similar procedure as described above.

Cloud point measurement

The cloud point temperatures (T_{cp} s) of the aqueous solutions of P[VBTP][Cl] of different molecular weights were determined in an UV-vis spectrophotometer equipped with a temperature controller in the transmittance mode at a fixed wavelength of $\lambda = 600$ nm. In a typical procedure, initially, we filtered a transparent aqueous solution of 0.5 wt% P[VBTP][Cl] through a membrane filter (pore size 0.45 μm). The solution was then titrated with NaCl to obtain a turbid solution at 25 °C. The resultant turbid solution was then taken in a 3 mL quartz cuvette and placed into a UV-vis spectrophotometer. The cloud point was then measured by recording the % transmittance (% T) in the temperature window of 10-90 °C with increasing/decreasing the temperature at 1 °C/min after equilibration for 2 min at the experimental temperature. Similarly, we measured the UCST-type cloud point of the aqueous solution of P[VBTP][Cl] of varying concentrations in presence of sodium halide salts. Moreover, T_{cp} s of 0.5 wt% of P[VBTP][Cl] solution of three different molecular weights were also determined in different concentrations of NaCl and NaBr salts and in different binary solvent mixtures such as water-MeOH, water-DMF and water-DMSO. The T_{cp} s were determined to be the point at which the solution transmittance reduced to half of its original value.

Preparation of cross-linked P[VBTP][Cl] hydrogel

For hydrogel preparation, [VBTP][Cl] (250 mg; 0.658 mmol), BIS (25 mg; 0.162 mmol) and ACVA (3.69 mg; 0.0131 mmol) were taken in a 15 mL glass vial and were dissolved in 1.665

mL H₂O and the reaction mixture was purged with dry argon for 30 min. Finally, the glass vial containing the reaction mixture was sealed with silicon rubber septum and was placed in an oil bath preheated at 70 °C and continued heating for 7 h to obtain a translucent gel.

Dispersion of MWCNTs in water using P[VBTP][Cl]

To obtain PIL-stabilized MWCNTs' dispersion in aqueous solution, the following experimental procedures were performed. MWCNTs (1 mg) was added into a vial containing 2 mL of an aqueous solution of P[VBTP][Cl]-40K (concentration 5 mg/mL). This mixture was sonicated for 7 h to obtain well-dispersed MWCNTs suspension, which was used for the study of thermoresponsiveness of PIL-adsorbed MWCNT in brine solution.

Characterization

¹H-NMR Study. ¹H-NMR spectra of the [VBTP][Cl] and P[VBTP][Cl] were acquired in a Bruker DPX 500 MHz spectrometer. CDCl₃ was used as solvent for acquiring the spectrum of [VBTP][Cl]. But, the spectrum of P[VBTP][Cl] was acquired from CDCl₃/CD₃OD (10:1) solvent mixture.

ESI Mass Spectrometry. ESI mass spectrum of the as-synthesized [VBTP][Cl] was recorded in a quadrupole time-of-flight (Q-TOF) Micro YA263 mass spectrometry. The sample was prepared at a concentration of 1mg/mL in methanol.

Fourier Transform Infrared (FTIR) Spectroscopy. FTIR spectra of [VBTP][Cl], P[VBTP][Cl] and P[VBTP][Cl]-MWCNT composite were recorded by mixing with KBr in 1:100 (w/w) ratio using a Spectrum 400 spectrometer (Perkin Elmer).

Gel Permeation Chromatography (GPC). The number average molecular weights (M_n) and polydispersities (PDI)s of the P[VBTP][Cl]s were measured by size exclusion chromatography using a Waters 1515 isocratic HPLC pump connected to two Waters Styragel HR3 and HR4 columns at 45 °C and a Waters 2414 RI detector at 35 °C. The eluent

was DMF with 50 mM LiBr, with a flow rate of 1 mL/min. The columns were calibrated against six poly(methyl methacrylate) standards with peak molecular weights (M_p) of 10100, 18700, 31600, 54500, 102000, and 174000.

Dynamic Light Scattering (DLS). DLS measurements were conducted using a light scattering apparatus equipped with a He-Ne laser Zetasizer NANO ZS 90, Malvern (Model 3690). The PIL solutions (0.5 wt%) were first filtered through a membrane filter of 0.45 μm pore size followed by addition of different halide salts prior to measurements. Measurements were carried out in the temperature range of 24 °C to 60 °C at a wavelength of 632.8 nm. The T_{cp} of 0.5 wt% aqueous P[VBTP][Cl]-40K with 475 mM NaCl solution was also determined from the abrupt change of hydrodynamic diameters (D_h) of aggregated PIL in a DLS instrument.

Field Emission Scanning Electron Microscopy (FESEM). A stable dispersion was prepared by dissolving 2 mg of P[VBTP][Cl]-40K in 2 mL of milli Q water containing 475 mM NaCl. The dispersed solution was then drop cast on small pieces of glass and allowed to dry overnight in air. The piece of glass containing the sample was then mounted on a metal stub followed by platinum coating to minimize charging. FESEM images were then acquired by placing the sample under a ZEISS JSM-6700F electron microscope operating at an accelerating voltage of 5 kV.

Transmission Electron Microscopy (TEM). For TEM study, one drop of aqueous dispersion of (0.01 wt%) of MWCNTs stabilized by P[VBTP][Cl]-40K was casted onto a carbon-coated copper grid and allowed to dried in air at room temperature for 24 h. The grid was then observed on a JEOL JEM-2010 electron microscope operated at an accelerating voltage of 200 kV.

Turbidity Measurements. The turbidity of aqueous solution of PIL was measured in a Hewlett Packard 8453 diode array UV-vis spectrophotometer (Agilent Technologies) equipped with a Peltier temperature controller.

Results and Discussion

Synthesis and characterization of [VBTP][Cl] monomer

As shown in Scheme 1, a phosphonium-based IL monomer, [VBTP][Cl] was synthesised by reaction of TPP with VBC. $^1\text{H-NMR}$ spectrum (Figure S1 in ESI) showed the characteristic signals at δ 7.04 and 7.10 ppm for phenyl ring protons of VBC and at δ 5.46 ppm for the benzylic $-\text{CH}_2$, next to the phosphonium cation. The well-resolved signals at δ 6.5, 5.6 and 5.2 ppm were attributed to the three vinyl protons of [VBTP][Cl] (Figure S1). Whereas the signals for three phenyl ring protons of TPP appeared at δ 7.57-7.75 ppm. All these signals confirmed the formation of [VBTP][Cl] monomer. The presence of only one sharp peak at m/z 379.11, which exactly matched with the molecular weight of the [VBTP][Cl] in the ESI mass spectrum (Figure S2) indicated that the monomer was free from impurities of the starting materials. The successful synthesis of [VBTP][Cl] monomer was further confirmed from the FTIR spectrum (Figure S3), which exhibited all its characteristic bands such as 1437 cm^{-1} (for deformation of P- CH_2 -Ph of [VBTP] $^+$), 1113 cm^{-1} (for three P-Ph stretching vibration) and 1627 cm^{-1} (for C=C stretching of vinyl bond).

Synthesis of P[VBTP][Cl] via RAFT polymerization

Conventional radical polymerization technique was frequently used to synthesize the thermoresponsive polymers^{33,35} compared to that prepared by, less reported, living polymerization methods.^{18,30} However, in this case, in order to prepare P[VBTP][Cl] of varying molecular weights, we employed RAFT polymerization of [VBTP][Cl] monomer. A versatile RAFT agent, CDP was used as CTA in combination with a radical initiator, AIBN for polymerization in DMF at $65\text{ }^\circ\text{C}$ (Scheme 1). We prepared P[VBTP][Cl]s of three different molecular weights by varying the $[[\text{VBTP}][\text{Cl}]_0]/[\text{CDP}]_0$ ratio and keeping the constant ratio of $[\text{CDP}]_0/[\text{AIBN}]_0 = 1:0.2$ as depicted in Table 1. Table 1 further revealed that the yields were reasonably good.

Table 1: Molecular characterization data of P[VBTP][Cl]s synthesized via RAFT polymerization.

Sample name	$[[\text{VBTP}][\text{Cl}]]_0/[\text{CDP}]_0$ $/[\text{AIBN}]_0$	Yield (%)	M_n (theo)	M_n (GPC)	<i>PDI</i>
P[VBTP][Cl]-40K	150:1:0.2	72	56900	40000	1.70
P[VBTP][Cl]-25K	100:1:0.2	76	37900	25000	1.62
P[VBTP][Cl]-18K	70:1:0.2	75	26500	18000	1.49

Reaction condition: Time = 24 h; Temperature = 65 °C; Solvent = DMF.

Usually, the GPC analysis of these cationic polymers were challenging because of their tendency to aggregate on the column fillers due the polymer-column interaction.^{41, 42} Indeed our first attempt to measure the molecular weights of P[VBTP][Cl]s using neat DMF as eluent was not successful as the chromatograms did not show any peak corresponding to these PILs. However, to overcome this problem, we used DMF containing 50 mM LiBr as an eluent at a column temperature of 45 °C. GPC traces shown in Figure 1 exhibited unimodal molecular weight distribution for three P[VBTP][Cl] samples with a lateral shifting towards higher elution time with the increase of molecular weight. As can be seen from the Table 1, the theoretical molecular weight M_n (theo) (calculated based on the $[[\text{VBTP}][\text{Cl}]]_0/[\text{CDP}]_0$ ratio) was slightly higher than the molecular weight obtained from GPC analysis with *PDI*s of 1.70, 1.62 and 1.49, which is little bit high considering RAFT polymerization technique. We do not know the exact reason for such high *PDI* values at this point. But, detailed study of RAFT polymerization of ionic liquid monomer is currently underway in our laboratory to explain such discrepancy.

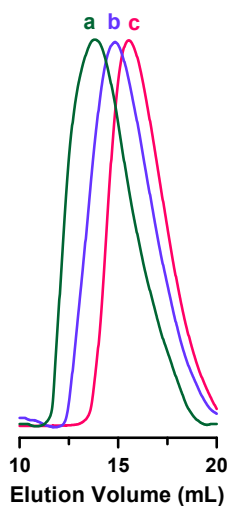


Figure 1. GPC traces of (a) P[VBTP][Cl]-40K, (b) P[VBTP][Cl]-25K and (c) P[VBTP][Cl]-18K prepared by RAFT polymerization. Eluent = DMF with 50 mM LiBr; Column temperature = 45 °C.

$^1\text{H-NMR}$ spectrum of a representative sample exhibited the absence of any signals corresponding to vinyl protons and the appearance of broad signals at δ 0.93-0.85 ppm corresponding to the backbone methylene and methine protons indicate the formation of pure P[VBTP][Cl] as shown in Figure S4. FTIR (Figure S3) was used to further characterise the P[VBTP][Cl]-40K, which revealed characteristic bands at 1659, 1510 and 1467 cm^{-1} corresponding to C=C stretching of phenyl group, 1436 cm^{-1} for P-CH₂ deformation, 1111 cm^{-1} for P-Ph stretching and 689 cm^{-1} for typical benzene ring out of plane bending. $^1\text{H-NMR}$ and FTIR results confirmed that the designed PIL can be conveniently prepared by one-step RAFT polymerization technique.

Temperature- and halide ion-responsiveness of P[VBTP][Cl] in aqueous solution

It has been reported that the thermoresponsive PILs generally exhibit LCST-type transition with a few exception that exhibiting UCST-type phase transition in aqueous solution.^{18, 33, 35}

Thus, we initially examined the temperature-dependent solution phase behavior of

P[VBTP][Cl] with an expectation that it would exhibit LCST-type transition in solution. Surprisingly, we found that this PIL was completely soluble in water (see the photograph in Scheme 2) as well as in various polar organic solvents such as MeOH, DMF and DMSO and the solution remained transparent over the temperature ranges of 0-90 °C. This result indicated that the PIL alone have no LCST- or UCST-type phase transition in those solvents within the above-mentioned temperature ranges. However, the transparent solution of P[VBTP][Cl] became opaque upon addition of small amount of sodium chloride at 25 °C as can be seen clearly from the photographs shown in Scheme 2. For optimization, we titrated a representative solution of P[VBTP][Cl]-40K (0.5wt%) with aqueous NaCl solution and found that the minimum concentration required to make the solution turbid at 25 °C (%T = 0.03) was 475 mM (Figure 2). It should be noted that the $[\text{NaCl}]_{\text{min}}$ (475 mM) required to make the solution turbid was independent of PIL concentration upto the tested concentration of 10 wt%. It was believed that the P[VBTP][Cl] molecules existed in soluble uncoiled state in water in absence of NaCl, but transformed into a collapsed globular state forming insoluble microgel aggregates in presence of NaCl. A possible mechanism is proposed to explain such behavior of P[VBTP][Cl] in solution with NaCl, which will be discussed later in this section. Furthermore, the turbid solution became transparent upon heating and the turbidity reappeared upon cooling indicating the presence of UCST-type phase transition (photographs shown in Scheme 2). The temperature-induced phase transitions of P[VBTP][Cl] solution was then examined in detail by slowly increasing the temperature (1 °C/min) of this cloudy P[VBTP][Cl]-40K solution (0.5wt %) and monitored the transmittance. The exact T_{cp} was determined from the transmittance versus temperature curve and was found to be 38 °C (Figure 2). This UCST-type of behavior was reversible under repeatable heating/cooling cycles for at least five times for all three PIL samples of different molecular weights as shown in Figure 3.

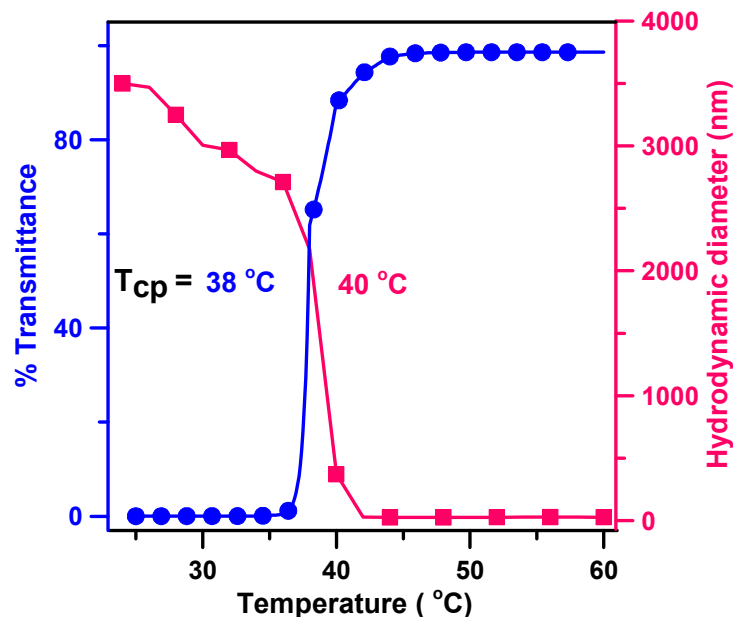


Figure 2. The correlation between hydrodynamic diameters (D_h)s (■) and % transmittance (at $\lambda = 600$ nm) (●) of aqueous P[VBTP][Cl]-40K solution (0.5wt%) with NaCl (475 mM) at different temperatures showing prominent cloud points.

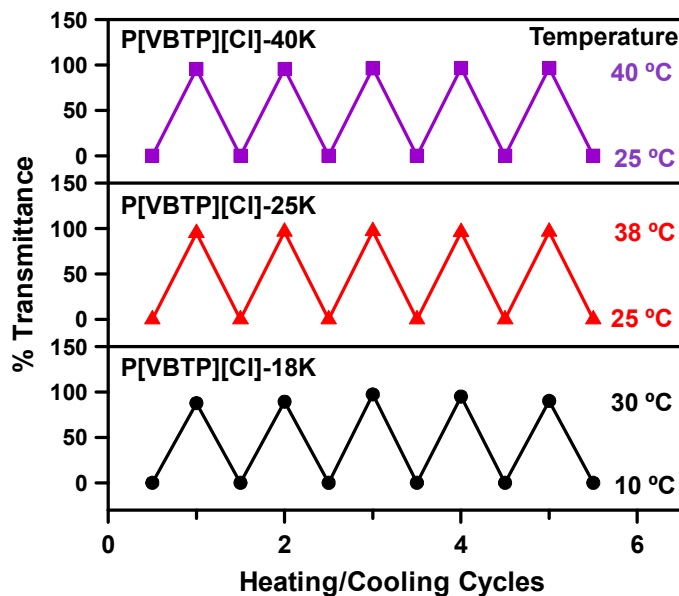


Figure 3. Temperature-dependent % transmittance of aqueous P[VBTP][Cl]s solutions of different molecular weights (0.5 wt% with 475 mM NaCl) during heating/cooling cycles. Each data point was obtained after equilibrating for 5 min.

The temperature-dependent phase transition of aqueous P[VBTP][Cl]-40K solution was further examined by DLS. The DLS data (Figure 2) showed that there was a rapid decrease in the hydrodynamic diameter (D_h) from 2174 to 27 nm as the temperature of the P[VBTP][Cl]-40K solution (0.5wt% with 475 mM NaCl) increased from 38 °C to 42 °C. Thus, it was further verified that with increase of temperature there was a transformation of two-phase system to one-phase system exhibiting a sharp UCST-type transition. The T_{cp} obtained from DLS was 40 °C, which was close to that (38 °C) obtained from turbidimetry (Figure 2). The D_h of the particles in the two-phase system of P[VBTP][Cl]-40K solution with 475 mM NaCl was 3200 nm at 25 °C (Figure S5), which is nothing but the microgel beads formed through PIL chain-chain interaction. The formation of microgel aggregates was further examined through FESEM study. An average diameter of spherical aggregates of 2500 nm was observed from FESEM image (Figure 4). The size of the formed microgel

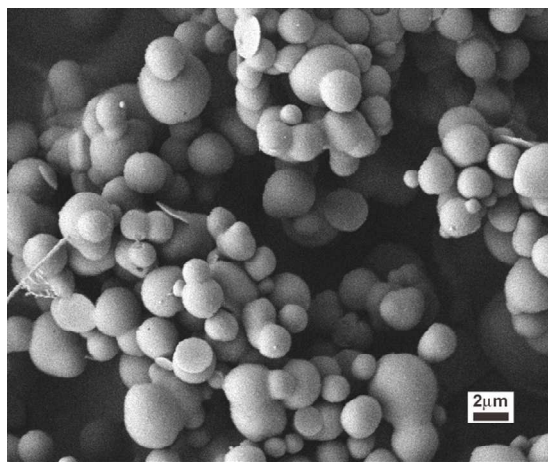
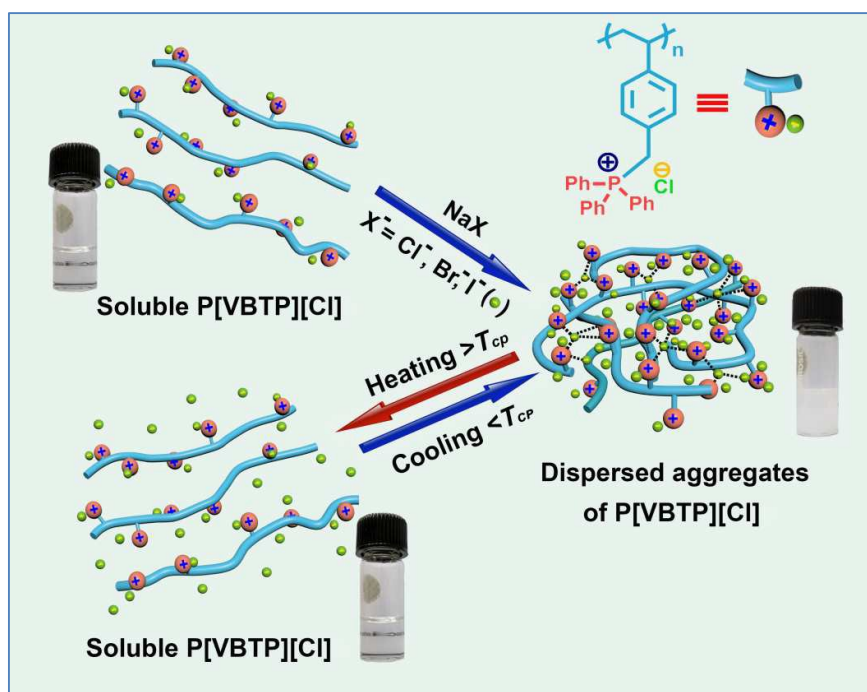


Figure 4. FESEM image of the aggregates of P[VBTP][Cl]-40K in aqueous solution (0.5wt % with 475 mM NaCl).

aggregates measured from FESEM image (2500 nm) was much lower than the D_h measured from DLS result (3200 nm). Usually such discrepancy in the size of aggregated particles is quite common, since the hydrodynamic diameter measured from DLS was actually the

hydrated diameter of the aggregated particles.^{30, 43} In this context, it should be mentioned that although the P[VBTP][Cl]-40K showed such thermoresponsiveness in aqueous solution, the corresponding [VBTP][Cl] monomer did not exhibit such behavior as checked by a control experiment.

The formation of microgel aggregates of P[VBTP][Cl] can be explained based on some literature reports on aggregation of some other PIL systems.^{28, 35, 42} According to those reports, there should be some kind of screening within the cationic charges of PIL chain in the presence of foreign anions. This effectively reduces the repulsive interaction between PIL chains and allows the individual chains to collapse into globular microgel state forming a two-phase system. Similarly, in this case, in presence of NaCl, the cationically charged pendent phosphonium groups of PIL were effectively screened by excess Cl⁻ ions and eventually made the PIL chains became hydrophobic in nature. The excess foreign Cl⁻ anion actually acts as a bridge between the neighbouring cationic P[VBTP]⁺ chains through the intra- and/or inter-molecular ionic crosslinking which would facilitates the extended PIL chains to aggregate into globular microgel beads (Scheme 2). This is the reason that the aqueous solution of P[VBTP][Cl] is responsive to Cl⁻. Furthermore, the weak ionic interaction between the Cl⁻ anions and the pendent cationic phosphonium ions can be disrupted by increasing the temperature, which converts the microgel beads into soluble uncoiled PIL chains indicating an UCST-type transition, resulting the P[VBTP][Cl] solution become doubly responsive (Scheme 2).



Scheme 2. Schematic representation of halide ion-induced soluble-insoluble and temperature-induced insoluble-soluble UCST-type phase transition of aqueous P[VBTP][Cl] solution. Inset shows the photographs of aqueous P[VBTP][Cl]-40K (0.5wt%) solution without NaCl at 25 °C (left), turbid solution below T_{cp} (right) and transparent solution above T_{cp} (middle-below).

Effect of nature of anions and their concentration on UCST-type cloud point

As mentioned above, the transparent P[VBTP][Cl] solution became turbid in presence of NaCl. Therefore, it would be really interesting to explore the phase behavior of this PIL solution in presence of other halide ions with varying concentrations. Accordingly, we observed that the transparent aqueous P[VBTP][Cl]-40K solution also became opaque upon addition of NaBr and NaI. The transparent P[VBTP][Cl]-40K (0.5wt %) solution became turbid only in presence of minimum of 20 mM NaBr, which was about 23 times lower than the $[\text{NaCl}]_{\text{min}}$ (475 mM) (described above) required to make the solution turbid at room temperature. Furthermore, for NaI, the minimum concentration was 2 mM, which was 10 times lower than $[\text{NaBr}]_{\text{min}}$ required to make such change. Also, in this case, we observed

precipitation and agglomeration of P[VBTP][Cl] from the aqueous solution. It should be further noted that the aqueous P[VBTP][Cl] solution did not turn into an opaque solution in presence of high F^- ion concentration (3M), which is expected because of its much lower size compared to the size of Cl^- . Thus, we may conclude that, the appearance of turbidity due to the formation of microgel bead of P[VBTP][Cl] largely dependent on the size of the anions which followed this order $I^- > Br^- > Cl^- > F^-$. As the size of the anion increases, the negative charge cloud becomes more dispersed and polarizable. Therefore, less number of polarizable anions can effectively interact with large number of cationic phosphonium groups of PIL chains, responsible for the agglomeration into microgel beads by screening the catatonically charged PIL chains. Hence, lower concentration was required for the larger anions to observe such type of phase transition.

Furthermore, we checked the effect of concentration of these halide ions on the T_{cp} s of aqueous P[VBTP][Cl] solution. We monitored the transmittance of 0.5wt% aqueous solution of three PIL samples (Table 1) in presence of varying amount of NaCl against temperature and the corresponding curves were given in Figure S6. Table S1 depicted the T_{cp} values of different samples under different NaCl concentrations. The transmittance curves of P[VBTP][Cl]-40K with NaBr of different concentrations were given in Figure S7 and the corresponding T_{cp} values were depicted in Table S2. A comparative plot (Figure 5) of the measured T_{cp} s against salt concentrations clearly revealed the linear increase of the T_{cp} s with increasing the concentration of both NaCl and NaBr. But, it was very clear from the slopes of these two lines in Figure 5 that the rate of increase of T_{cp} against concentration of NaBr was about 2.5 times higher than that of NaCl. However, in case of NaI, the interaction among the PIL chains through I^- ion (2 mM) is so high that the formed microgel could not acquire sufficient energy to rupture upon heating upto ~ 90 °C. Thus the effect of halide ion concentration on the T_{cp} also followed the same order as observed in the case of turbidity

formation of P[VBTP][Cl] in solution caused by their polarizability differences. With the increase of salt concentration, the larger anions with high polarizability interact strongly with the more number of cationic phosphonium groups of the PIL chains than the smaller one with less polarizability, which is actually reflected in the slopes of these lines in Figure 5.

We also checked anion-responsive phase behavior of P[VBTP][Cl] solution in presence of cyanide (CN^-) and thiocyanate (SCN^-) anions. We found that the transparent P[VBTP][Cl]-40K (0.5wt%) solution became turbid in presence of minimum of 5 mM SCN^- and 350 mM CN^- . But, these turbid solutions did show any transition (insoluble-soluble) upon heating upto a temperature $\sim 90^\circ\text{C}$.

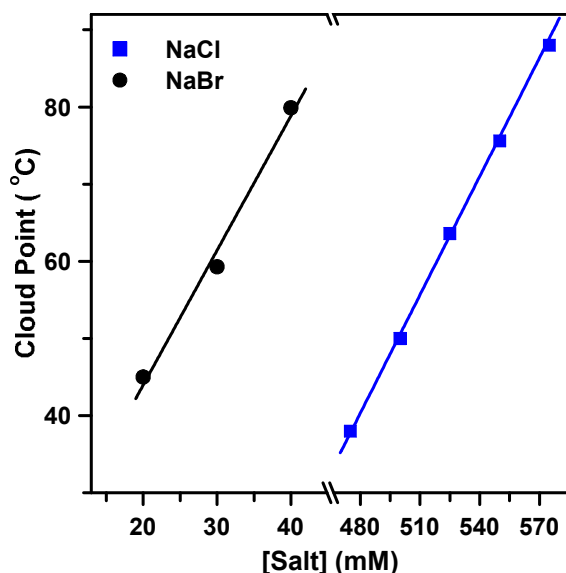


Figure 5. Plot of T_{cps} as a function of NaCl and NaBr concentration for 0.5 wt% aqueous P[VBTP][Cl]-40K solution.

Effects of molecular weight and concentration of PIL on cloud point

To check the effect of molecular weight on T_{cp} , we systematically monitored the transmittance of cloudy solution of three samples, P[VBTP][Cl]-40K, P[VBTP][Cl]-25K and P[VBTP][Cl]-18K (Table 1) with increasing temperature in presence of 500 mM NaCl. The transmittance curves of three samples exhibited a sharp UCST-type transition at different

temperatures with reversibility (Figure 6). These curves clearly showed that the T_{cp} increases with increase of their molecular weights (see Table S1). The variation of T_{cp} values of these three samples at other NaCl concentrations also followed the same trend as observed in presence of 500 mM NaCl (see Table S1). Such observation is quite common for other thermoresponsive polymeric system.^{29, 30, 44} As the molecular weight of P[VBTP][Cl] increased, the number of cationic centres in the PIL chain also increased resulting in more intra- and/or inter-molecular ionic bridging at a fixed anion concentration. Hence, higher energy is required to disrupt such interaction, which increases the T_{cp} of P[VBTP][Cl] solution.

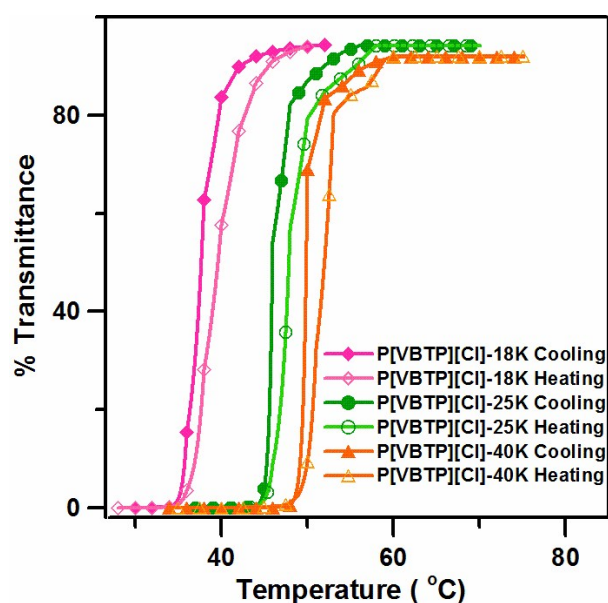


Figure 6. Transmittance curves of 0.5 wt% aqueous solution of P[VBTP][Cl] of different molecular weights containing 500 mM NaCl during heating/cooling cycles.

We further investigated the effect of concentration of P[VBTP][Cl]-40K on its UCST-type cloud points and the transmittance curves were given in Figure 7A. The curves revealed that the T_{cp} had a strong dependency on PIL concentration at fixed NaCl concentration of 475 mM. From the curve (Figure 7B), it was clear that the T_{cp} initially increased with PIL concentration and reached a maximum at a concentration of 6 wt% and then it showed a

decreasing trend. But, we were unable to measure the T_{cp} of this PIL solution having concentration more than 10 wt% because of high viscosity of the solution. These results again suggested that intra- and/or inter-molecular ionic interactions through the ion bridging are responsible for such phase transition behavior. With increasing PIL concentration from 0.1 to 6wt%, the developing ionic bridging density predominates over cationic repulsion among PIL chains, whereas above 6wt% ionic repulsion override the developing ionic bridging density, resulting in such phase diagram as shown in Figure 7B.

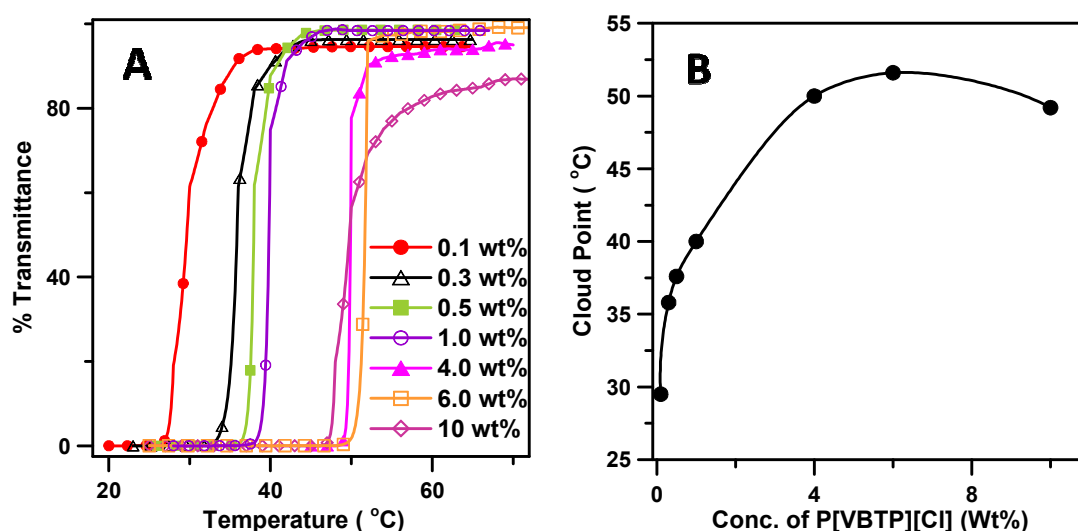


Figure 7. (A) Transmittance cooling curves of aqueous solutions of P[VBTP][Cl]-40K containing 475 mM NaCl and (B) Dependence of T_{cp} on P[VBTP][Cl]-40K concentration in the presence of 475 mM NaCl.

Thermoresponsiveness of P[VBTP][Cl] in binary mixtures of water with other organic cosolvents

It was mentioned above that, P[VBTP][Cl] was soluble in water, MeOH, DMF, DMSO but exhibited an UCST-type phase transition in water in presence of halide ion. Hence, we investigated the thermosensitiveness of a representative sample, P[VBTP][Cl]-40K in the binary mixture of water-MeOH, water-DMF and water-DMSO to check whether there is any

effect of solvent polarity. We measured the transmittance of P[VBTP][Cl]-40K (0.5 wt%) solution in these binary mixtures of varying cosolvent compositions (Figure S8) with temperature and measured the T_{cp} values. We noticed that, the T_{cp} (75.6 °C) of P[VBTP][Cl]-40K (0.5 wt % with 550mM NaCl) in water decreased linearly with increasing volume% of MeOH in water-MeOH mixed solvent (Figure 8). Further, it was also observed that the T_{cp} similarly decreased linearly with increasing volume% of DMF and DMSO in the mixed solvent system (Figure 8). It should be noted from Figure 8 that the rate of decrease of T_{cp} with increase of volume% of DMF or DMSO was sharper compared to that of increase of volume% of MeOH. But, in the cases of DMF or DMSO as cosolvent, the rates of decrease of T_{cp} with increase of volume% of these solvents were almost the same. Such decrease of cloud point of P[VBTP][Cl] in mixed solvents can be explained with help of their donor number (DN), which is a nothing but the measure of their electron donation property. It has been reported that the DN of these solvents follows this order $DMSO \geq DMF > MeOH$.⁴⁵ The DN of the solvent also influenced the donicity of anion towards the cation of an ionic liquid⁴⁶ and would follow the same order as mention above. In this case, thus, the presence of these

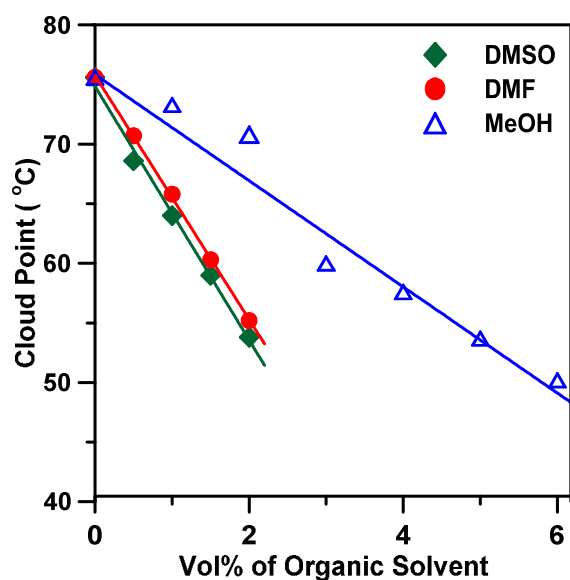


Figure 8. Effect of organic cosolvent composition on the T_{cps} of P[VBTP][Cl]-40K (0.5 wt%) in water-organic solvent binary mixture containing 550 mM NaCl .

solvents actually affect the donicity of Cl^- anion towards the phosphonium cation of P[VBTP][Cl]. Solvent of higher DN, such as DMSO/DMF would replace the excess Cl^- ion acting as a bridge between phosphonium ions of PIL chains more than the solvent of lower DN, such as MeOH. This is the reason why we observed different rate of decrease of T_{cp} of the P[VBTP][Cl] in mixed solvents in presence of different cosolvents (Figure 8).

Dual responsive cross-linked hydrogel

Thermoresponsive hydrogels have been the topic of extensive research in the field of pharmaceutical and biomedical science recently.⁴⁷ Thus, we aimed to prepare PIL-based hydrogel systems that can response to temperature. In order to do this, we synthesized a cross-linked hydrogel of P[VBTP][Cl]-40K containing 10 wt% N, N'-methylenebis(acrylamide) (BIS) as the cross-linker. This hydrogel was initially transparent when swelled with water (Figure 9A). The swelled hydrogel was then immersed into a solution of 0.9 (M) NaCl until it deswelled to an opaque and squeezed gel (Figure 9B). It was observed through naked eye that the shrunk turbid gel start to reswell rapidly when the temperature was slowly increased to 70 °C and eventually transformed into a transparent gel as can be seen clearly from the photographs given in Figure 9C. It was observed that this P[VBTP][Cl]-based cross-linked hydrogel needed higher NaCl concentration to obtain opaque gel than that required for uncross-linked neat P[VBTP][Cl] solution to become turbid.

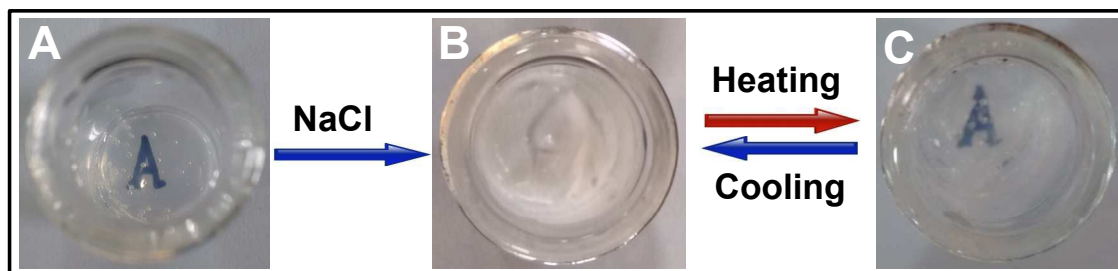


Figure 9. Cross-linked hydrogel of P[VBTP][Cl]-40K in H_2O : (A) Transparent gel at 25 °C; (B) Squeezed opaque gel at 25 °C with 0.9 M NaCl; (C) Transparent gel at 70 °C with 0.9 M NaCl.

This may be ascribed to higher concentration of the P[VBTP][Cl] in the gel state. Furthermore, the role of the presence of BIS cross-linker in the gel cannot be ruled out. The detailed investigation of effect of cross-linker on the thermosensitiveness of this hydrogel is underway in our laboratory. Earlier, Boyko et al. was observed similar type of thermoresponsive swelling/reswelling behaviors of cross-linked PHEMA and PNIPAM gels in water-alcohol solution.⁴⁸

Double responsiveness of P[VBTP][Cl]-stabilized MWCNTs in water

In this case, we try to utilize this cationic P[VBTP][Cl] for making stable dispersion of MWCNTs in water. We found that the P[VBTP][Cl]-40K can efficiently stabilize MWCNTs dispersions in water. The dispersion was black in color and was remained stable upto 72 h without any precipitation (Figure 10). The FTIR spectrum (Figure S9) of P[VBTP][Cl]-40K-MWCNTs composite showed the characteristic bands at 1437 cm^{-1} (for deformation of P- CH_2Ph of $[\text{VBTP}]^+$), 1111 cm^{-1} (for P-Ph stretching vibration) and 689 cm^{-1} (for benzene ring out of plane bending) indicating the successful adsorption of P[VBTP][Cl] on MWCNTs' surface. For further confirmation, we also examined the P[VBTP][Cl]-stabilized MWCNTs' dispersion via transmission electron microscopy (TEM). Mostly individual nanotubes were observed in the TEM image (Figure 11), pointing out that P[VBTP][Cl] had a fairly good

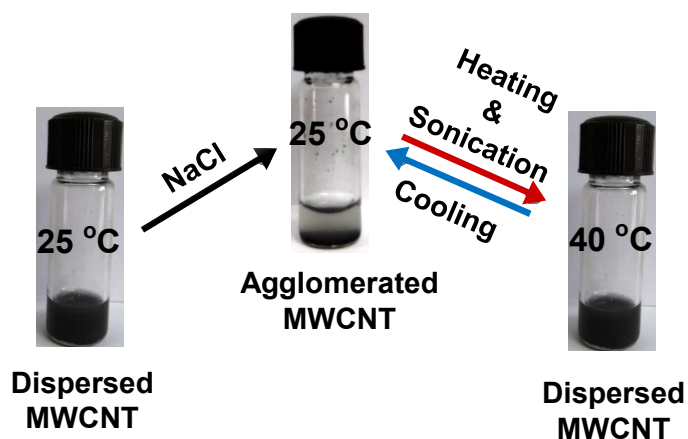


Figure 10. Photographs of dual responsiveness of P[VBTP][Cl]-40K-stabilized MWCNT dispersion in water.

unbundling activity on aggregated MWCNTs. Moreover, the enlarged view of a side portion of a single nanotube clearly revealed a dark core and a lighter amorphous corona of thickness 10.7 nm, which was nothing but P[VBTP][Cl] layer. However, the core clearly showed the crystalline fringes of CNT with a spacing of 0.34 nm between two fringes, which exactly matched with the reported value.⁴⁹

Furthermore, the stimuli-responsiveness of adsorbed P[VBTP][Cl]-40K in aqueous NaCl solution was utilized for the temperature-induced aggregation and exfoliation of MWCNTs. We first prepared a stable dispersion of MWCNTs using P[VBTP][Cl]-40K (0.5 wt%). Addition of 475 mM NaCl into this dispersion resulted in the agglomeration of MWCNTs from its stable aqueous dispersion. The aggregation of the adsorbed P[VBTP][Cl]-40K molecule upon addition of NaCl actually forced to agglomerate the dispersed MWCNTs at 25 °C. It was mentioned above that the P[VBTP][Cl]-40K (0.5 wt%) in presence of 475 mM NaCl exhibited a UCST-type phase transition at 38 °C. Thus, the agglomerated P[VBTP][Cl]-40K-MWCNTs can again be back into dispersion in water upon ultrasonication for 5 min and heating at 40 °C (Figure 10). Heating provides sufficient energy to solubilise

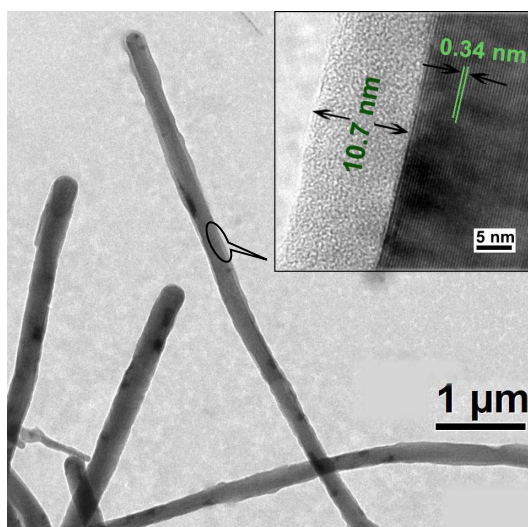


Figure 11. TEM image of MWCNTs stabilized with P[VBTP][Cl]-40K in water.

the collapsed P[VBTP][Cl] that were adsorbed on MWCNTs, by disrupting the ionic interactions. This results in a dispersion of P[VBTP][Cl]-adsorbed MWCNTs in water. This observation was totally reversible for several times. In this context, it should be mentioned that recently, a thermoresponsive anionic PIL³³ and a copolymer of PNIPAM and an imidazolium PIL⁵⁰ with LCST-type phase transition were used for the dispersion of CNT below the cloud point. There also precipitation and redispersion reversibly observed for the adsorption of LCST-type PIL on the CNT surface through cation- π interaction. In contrast, this work represented a phosphonium PIL having tunable UCST-type phase transition induced a transition of agglomerated MWCNTs to its exfoliated state in water above the cloud point.

Conclusions

In summary, we employed RAFT polymerization to synthesize cationic poly(ionic liquid), poly(triphenyl-4-vinylbenzylphosphonium chloride)s (P[VBTP][Cl])s of varying and controllable molecular weights showing double responsiveness towards halide ions and temperature (UCST-type) in aqueous solution. Upon addition of halide ion, the transparent P[VBTP][Cl] solution became a two-phase system owing to the generation of insoluble microgel aggregates formed through intra- and/or inter-chain crosslinking of phosphonium cations of P[VBTP][Cl] by halide anion bridging. The minimum concentration of halide ion required for the aggregation of P[VBTP][Cl] (appearance of turbidity) was largely dependent on their sizes and the order was $\Gamma^- > \text{Br}^- > \text{Cl}^-$. Upon heating, the aggregated two-phase system transformed into one-phase system above the T_{cp} , showing a distinct UCST-type phase transition as examined by DLS and turbidimetry. It was found that the UCST-type T_{cp} of P[VBTP][Cl] increased with increasing its molecular weight. This was further supported by the fact that the cloud point temperature could be easily tuned in a vast temperature window

in terms of PIL concentration, nature and concentration of halide ions. T_{cp} of P[VBTP][Cl] showed decreasing trend upon increasing concentration of organic cosolvent in the binary mixture with water. The P[VBTP][Cl] was successfully employed to prepare a double responsive cross-linked hydrogel and was applied as a smart stabilizer to promote water borne double-responsive dispersion of MWCNTs towards halide ions and temperature. This opens up the possibility of making environment-responsive gel material and carbon nanostructures' dispersion

Acknowledgements

Y.B. thanks IACS for providing fellowship. T. M. and M. D. thank CSIR for fellowship. This research was supported by the grants from CSIR, New Delhi. Thanks are also due to the partial financial support from BRNS, India.

Electronic Supplementary Information (ESI): Tables summarizing the effect of addition of NaCl/NaBr on UCST-type cloud point, $^1\text{H-NMR}$ and FTIR spectra of [VBTP][Cl] and P[VBTP][Cl]-40K, ESI mass spectrum of [VBTP][Cl], DLS data of P[VBTP][Cl]-40K, transmittance curves showing the effect of NaCl and NaBr salt concentration and the effect of organic cosolvent composition on cloud points of P[VBTP][Cl]-40K, FTIR spectra of P[VBTP][Cl]-40K-MWCNT composite. This material is available free of charge via the Internet at <http://pubs.rsc.org>.

Notes and References

1. O. Green, S. Grubjesic, S. Lee and M. A. Firestone, *Polym. Rev.*, 2009, **49**, 339-360.
2. J. Lu, F. Yan and J. Texter, *Prog. Polym. Sci.*, 2009, **34**, 431-448.

3. D. Mecerreyes, *Prog. Polym. Sci.*, 2011, **36**, 1629-1648.
4. J. Yuan and M. Antonietti, *Polymer*, 2011, **52**, 1469-1482.
5. J. Yuan, D. Mecerreyes and M. Antonietti, *Prog. Polym. Sci.*, 2013, **38**, 1009-1036.
6. T. P. Fellingner, A. Thomas, J. Y. Yuan and M. Antonietti, *Adv. Mater.*, 2013, **25**, 5838-5854.
7. W. J. Horne, M. A. Andrews, K. L. Terrill, S. S. Hayward, J. Marshall, K. A. Belmore, M. S. Shannon and J. E. Bara, *ACS Appl. Mater. Interfaces*, 2015, **7**, 8979-8983.
8. R. Marcilla, E. Ochoteco, C. Pozo-Gonzalo, H. Grande, J. A. Pomposo and D. Mecerreyes, *Macromol. Rapid Commun.*, 2005, **26**, 1122-1126.
9. H. Ohno and K. Ito, *Chem. Lett.*, 1998, **27**, 751-752.
10. F. Yan and J. Texter, *Angew. Chem. Int. Ed.*, 2007, **119**, 2492-2495.
11. J. T. Yang, J. Z. Zheng, J. J. Zhang, L. Sun, F. Chen, P. Fan and M. Q. Zhong, *RSC Adv.*, 2015, **5**, 32853-32861.
12. M. Yoshizawa and H. Ohno, *Chem. Lett.*, 1999, **28**, 889-890.
13. J. Yuan, C. Giordano and M. Antonietti, *Chem. Mater.*, 2010, **22**, 5003-5012.
14. Y. Kohno, S. Saita, Y. J. Men, J. Y. Yuan and H. Ohno, *Polym. Chem.*, 2015, **6**, 2163-2178.
15. R. Cheng, F. Meng, C. Deng, H. A. Klok and Z. Zhong, *Biomaterials*, 2013, **34**, 3647-3657.
16. P. Schattling, F. D. Jochum and P. Theato, *Polym. Chem.*, 2014, **5**, 25-36.
17. J. Seuring and S. Agarwal, *Macromol. Rapid Commun.*, 2012, **33**, 1898-1920.
18. H. Yoshimitsu, A. Kanazawa, S. Kanaoka and S. Aoshima, *Macromolecules*, 2012, **45**, 9427-9434.
19. A. Hatefi and B. Amsden, *J. Control. Release*, 2002, **80**, 9-28.

20. S. A. Asher, M. Kamenjicki, I. K. Lednev and V. Meier, United States Patent, 2001.
21. Y. Kumashiro, M. Yamato and T. Okano, *Ann Biomed Eng.*, 2010, **38**, 1977-1988.
22. D. Cunliffe, C. de las Heras Alarcon, V. Peters, J. R. Smith and C. Alexander, *Langmuir*, 2003, **19**, 2888-2899.
23. H. G. Schild, *Prog. Polym. Sci.*, 1992, **17**, 163-249.
24. R. A. Horne, J. P. Almeida, A. F. Day and N.-T. Yu, *J. Colloid Interface Sci.*, 1971, **35**, 77-84.
25. S. Aoshima, H. Oda and E. Kobayashi, *J. Polym. Sci., Part A: Polym. Chem.*, 1992, **30**, 2407-2413.
26. R. Hoogenboom, *Angew. Chem. Int. Ed.*, 2009, **48**, 7978-7994.
27. O. V. Klenina and E. G. Fain, *Polym. Sci. U.S.S.R.*, 1981, **23**, 1439-1446.
28. F. A. Plamper, A. Schmalz and A. H. E. Muller, *J. Am. Chem. Soc.*, 2007, **129**, 14538-14539.
29. N. Shimada, H. Ino, K. Maie, M. Nakayama, A. Kano and A. Maruyama, *Biomacromolecules*, 2011, **12**, 3418-3422.
30. T. Maji, S. Banerjee, Y. Biswas and T. K. Mandal, *Macromolecules*, 2015, **48**, 4957-4966.
31. S. Amajjahe and H. Ritter, *Macromolecules*, 2008, **41**, 3250-3253.
32. E. Karjalainen, V. Aseyev and H. Tenhu, *Macromolecules*, 2014, **47**, 7581-7587.
33. Y. Men, X.-H. Li, M. Antonietti and J. Yuan, *Polym. Chem.*, 2012, **3**, 871-873.
34. Y. J. Men, M. Drechsler and J. Yuan, *Macromol. Rapid Commun.*, 2013, **34**, 1721-1727.
35. Y. Men, H. Schlaad and J. Yuan, *ACS Macro Lett.*, 2013, **2**, 456-459.
36. M. Tunckol, E. Zuza-Hernandez, J. R. Sarasua, J. Durand and P. Serp, *Eur. Polym. J.*, 2013, **49**, 3770-3777.

37. M. Antonietti, Y. Shen, T. Nakanishi, M. Manuelian, R. Campbell, L. Gwee, Y. A. Elabd, N. Tambe, R. Crombez and J. Texter, *ACS Appl. Mater. Interfaces*, 2010, **2**, 649-653.
38. R. Marcilla, M. L. Curri, P. D. Cozzoli, M. T. Martínez, I. Loinaz, H. Grande, J. A. Pomposo and D. Mecerreyes, *Small*, 2006, **2**, 507-512.
39. L. Zhao, R. Crombez, F. P. r. Caballero, M. Antonietti, J. Texter and M.-M. Titirici, *Polymer*, 2010, **51**, 4540-4546.
40. B. Dong, Y. Su, Y. Liu, J. Yuan, J. Xu and L. Zheng, *J. Colloid Interface Sci.*, 2011, **356**, 190-195.
41. H. He, M. Zhong, B. Adzima, D. Luebke, H. Nulwala and K. Matyjaszewski, *J. Am. Chem.Soc.*, 2013, **135**, 4227-4230.
42. R. Longenecker, T. Mu, M. Hanna, N. A. D. Burke and H. D. H. Stover, *Macromolecules*, 2011, **44**, 8962-8971.
43. T. Das, T. K. Paira, M. Biswas and T. K. Mandal, *J. Phys. Chem. C*, 2015, **119**, 4324-4332.
44. J. Seuring and S. Agarwal, *Macromolecules*, 2012, **45**, 3910-3918.
45. V. Gutmann, ed., *The Donor– Acceptor Approach to Molecular Interactions*, Springer, 1978.
46. M. Holzweber, R. Lungwitz, D. Doerfler, S. Spange, M. Koel, H. Hutter and W. Linert, *Chem. Euro. J.*, 2013, **19**, 288-293.
47. L. Klouda and A. G. Mikos, *Eur. J. Pharm. Biopharm.* , 2008, **68**, 34-45.
48. V. Boyko, Y. Lu, A. Richter and A. Pich, *Macromol. Chem. Phys.*, 2003, **204**, 2031-2039.
49. O. V. Kharissova and B. I. Kharisov, *RSC Adv.*, 2014, **4**, 30807-30815.
50. S. Soll, M. Antonietti and J. Yuan, *ACS Macro Lett.*, 2011, **1**, 84-87.

Table of Contents

Tunable Doubly Responsive UCST-Type Phosphonium Poly(ionic liquid): A Thermosensitive Dispersant for Carbon Nanotubes

Yajnaseni Biswas, Tanmoy Maji, Madhab Dule and Tarun K. Mandal*

Poly(triphenyl-4-vinylbenzylphosphonium chloride) synthesized via RAFT polymerization exhibits both tunable halide ion- and thermo-responsiveness (UCST-type) in aqueous solution and acts as a thermosensitive stabilizer for carbon nanotubes.

